Dynamic Modeling of Biped Robot using Lagrangian and Recursive Newton-Euler Formulations

Hayder F. N. Al-Shuka
Baghdad University,Mech. Eng. Dep.,Iraq

Burkhard J. Corves
RWTH Aachen University, IGM, Germany

Wen-Hong Zhu
Canadian Space Agency, Canada

ABSTRACT

The aim of this paper is to derive the equations of motion for biped robot during different walking phases using two well-known formulations: Euler-Lagrange (E-L) and Newton-Euler (N-E) equations. The modeling problems of biped robots lie in their varying configurations during locomotion; they could be fully actuated during the single support phase (SSP) and over-actuated during the double support phase (DSP). Therefore, first, the E-L equations of 6-link biped robot are described in some details for dynamic modeling during different walking phases with concentration on the DSP. Second, the detailed description of modified recursive Newton-Euler (N-E) formulation (which is very useful for modeling complex robotic system) is illustrated with a novel strategy for solution of the over-actuation/discontinuity problem. The derived equations of motion of the target biped for both formulations are suitable for control laws if the analyzer needs to deal with control problems. As expected, the N-E formulation is superior to the E-L concerning dealing with high degrees-of-freedom (DoFs) robotic systems (larger than 6 DoFs).

General Terms

Multibody dynamics, Robotics, Biped robots.

Keywords

Biped robots, Lagrangian formulation, Recursive Newton-Euler formulation, dynamics.

1. INTRODUCTION

Humans have perfect mobility with amazing control systems; they are extremely versatile with smooth locomotion. However, comprehensive understanding of the human locomotion is still not entirely analyzed. To dynamically model the ZMP-based biped mechanisms, the following points should be taken into consideration:

i. The biped robots are kinematically varying mechanisms such that they could be fully actuated during the SSP and over-actuated during DSP. If we assume the biped robot as fixed-base mechanism, the dynamic modeling and control strategies of fixed-base manipulators can be used efficiently.

ii. Dealing with unilateral contact of the foot-ground interaction as a passive joint (rigid-to-rigid contact) or as compliant model (penalty-based approach), see [1].

iii. Reducing the number of links/joints of the target biped as possible. But, they can still have more than 6 DoFs resulting in computational problems of advanced control systems.

iv. Reducing the walking phases as much as possible. In general, the designer could select one or more of the walking patterns discussed in [2] according to her/his aim, e.g., most conventional ZMP-based biped robots can walk with two substantial walking phases: the SSP

and the DSP. Adjustments of the walking patterns are possible by modification of foot design as described in [3].

v. Most ZMP-based biped robots walks with flat swing /stance feet all the time; this can facilitate the analysis of biped locomotion by reducing walking phases to exactly two phases: the SSP and the DSP (see [4]). However, heel-off/toe-off sub-phases can offer better characteristics but with careful analysis.

In the light of the above comments, the classical E-L equations and recursive N-E can be used for dynamic modeling of biped robots. For complex robotic systems, such as humanoid robots or any robot having the number of DoFs larger than 6 DoFs, difficulties are encountered in the implementation of the control algorithms. Therefore, over 30 years, the robotics researchers have focused on the problem of computational efficiency. Many efficient O (n) algorithms have been developed for inverse and forward dynamics of robotic systems. For more literature on the efficient dynamic algorithms, refer to refs. [5-7]. The adaptive control algorithm, however, which deals with controlling the robotic systems despite their uncertain parameters may decrease the computational efficiency of the dynamics O (n) algorithms. Fu et al. [8] have shown that the combined identification and control algorithms can be computed in O (n^3) time despite using the recursive N-E formulation. One of the efficient tools to deal with full-dynamics-based control for complex robotic systems is the virtual decomposition control (VDC) suggested by Wen-Hong Zhu [9]. It is equivalent to the recursive N-E formulation if the dynamic parameters of the target robotic system are known.

This paper deals with the ZMP-based biped robot as a fixed-base robot with rigid foot-ground interaction. In addition, E-L equations are described in some details for dynamic modeling of the biped during different walking phases; problems of over-actuation/ discontinuity are resolved. Then detailed description of the N-E formulation is illustrated with a novel strategy for solution of the over-actuation/discontinuity problem. The remainder of this paper is organized as follows. Selection of the walking patterns suggested throughout the current paper is presented in Section 2 Section 3 deals with detailed modeling of biped robot using the E-L equations and N-E formulations. Section 4 concludes.

2. WALKING PATTERNS

The complete gait cycle of human walking consists of two main successive phases: DSP and SSP with intermediate sub-phases. The DSP arises when both feet contact the ground resulting in a closed chain mechanism while SSP starts when the rear foot swings in the air with the front foot flat on the ground. Different walking patterns can be selected for the design of biped locomotion as detailed in [2, 10]. However, the walking pattern described in Figure 1 will be adopted in

this paper. It consists of one SSP and two sub-phases of the DSP. In the first sub-phase of the DSP (henceforth called DSP1), the front foot starts to rotate about the heel tip until it will be level to the ground. The rear foot, meanwhile, is in full contact with the ground. Then the rear foot will rotate about the front edge in the second sub-phase of the DSP (henceforth called DSP2).
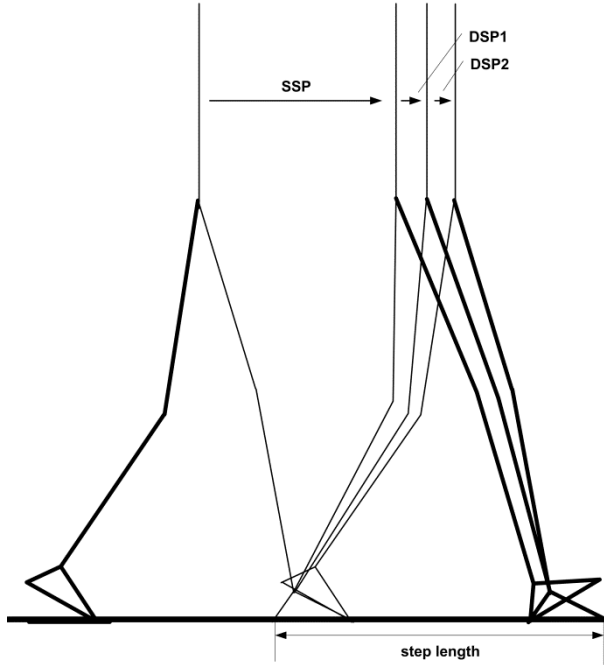

Fig. 1:The selected walking pattern of the biped robot

3. DYNAMIC MODELING

This paper concentrates on formulating the dynamic equations that are suitable for adaptive control purposes. Throughout the current analysis, the following assumptions have been proposed.

Assumption 1. The stance foot is in full contact with the ground during the SSP; therefore, its dynamics could be neglected in such case. This assumption is necessary for ZMP-based stability.

Assumption 2. The foot-ground contact is rigid-to-rigid contact. Accordingly, the tips of the feet (in case of foot rotation) are assumed passive joints.

Assumption 3. There are only two substantial walking phases, the SSP and the DSP, with possibly sub-phases during the DSP. The instantaneous impact event is avoided by making the swing foot contact the ground with zero velocity.

In biped systems, three important aspects should be taken into consideration [11]

   (i)   Preventing the biped legs from slippage.

   (ii) Avoiding discontinuities of the ground reaction forces which can result in discontinuities of the actuator torques.

   (iii) Concentrating on the adaptive control of the biped robot associated with less computational complexity.

3.1 The Euler-Lagrange formulation

Although the E-L equations can provide closed-form state equations suitable to advanced control strategies, their computational complexity, unless it is simplified, could be inefficient for analysis/control of complex robotic system (more than 6 DoFs) [9]. Below we present modeling of biped robot during the two phases: the SSP and the DSP with two different kinds of Lagrange equations.

3.1.1 E-L equations of the second kind (the SSP)

The E-L equations for open chain mechanism (biped robot during the SSP as shown in Figure 2) can be expressed as

$$\frac{d}{dt}\left(\frac{\partial L}{\partial \dot{q}_i}\right) - \frac{\partial L}{\partial q_i} = T_i \quad (i = 1, 2, \dots \dots, n_q) \tag{1}$$

where L is Lagrangian function which is equal to the kinetic energy of the robotic system (K) minus its potential energy (P), q_i denotes the generalized coordinates of link (i), and $\dot{q}_i$ is the derivative of the generalized coordinates.
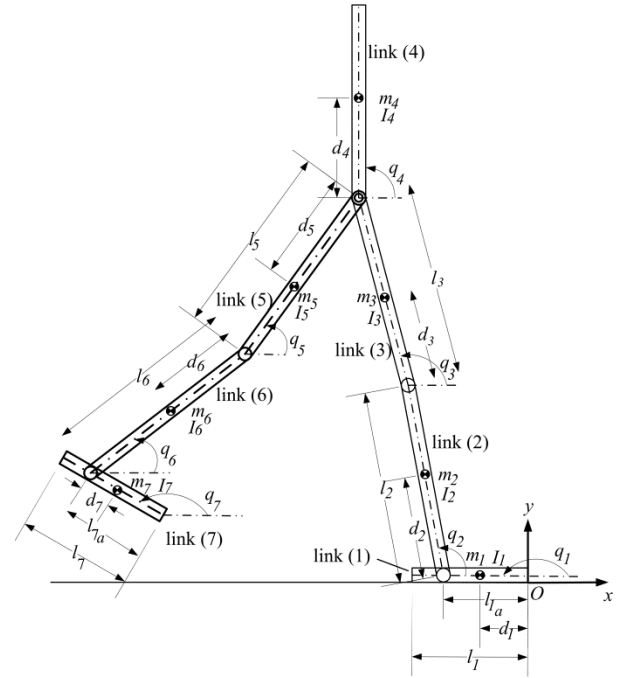

Fig. 2:The biped configuration during the SSP

The generalized coordinates are a set of coordinates that completely describes the location (configuration) of the dynamic systems relative to some reference configuration [8]. There are many choices to select these generalized coordinates; however, the joint/link displacements are proved being suitable in case of robotic systems. If the number of these generalized coordinates is equal to the degrees of freedom of the target system, then (1) is valid; (1) is called Lagrange equations of the second kind and it suitable for open-chain mechanism. Solution of (1) can result in the following second order differential equations.

$$M(q)\ddot{q} + C(q,\dot{q})\dot{q} + g(q) = A(\tau - \tau_f) \tag{2}$$

or simply,

$$M(q)\ddot{q} + C(q,\dot{q})\dot{q} + g(q) + A\tau_f = A\tau \tag{3}$$

where $M \in \mathbb{R}^{n_q \times n_q}$ is the mass matrix, q, $\dot{q}$ and $\ddot{q} \in \mathbb{R}^{n_q}$ are the absolute angular displacement, velocity and acceleration of the robot links, $C \in \mathbb{R}^{n_q \times n_q}$ represents the Coriolis and centripetal robot matrix, $g \in \mathbb{R}^{n_q \times 1}$ is the gravity vector, $A \in \mathbb{R}^{n_q \times n_\tau}$ is a mapping matrix derived by the principle of the virtual work [12, 13], $\tau \in \mathbb{R}^{n_\tau \times 1}$ is the actuating torque vector, n_τ represents the number of actuators, and $\tau_f \in \mathbb{R}^{n_\tau \times 1}$.represents the dissipative torques resulted from joint friction.

Remark 1. There are several fundamental properties of the dynamic coefficient matrices, the mass matrix and the Coriolis and centripetal terms, which could be exploited in controller design of adaptive control; for more details on other properties, refer to [14, 15].

Property 1. The mass matrix (M) is symmetric and positive definite. This can be deduced from the property of the kinetic energy.

Property 2. The matrix $\dot{M}(q) - 2C(q,\dot{q})$ is skew matrix, if the $C(q,\dot{q})$ matrix is described in terms of Christoffel symbols.

Property 3. The dynamic equations described in (2) are dependent linearly on certain parameters such as link masses, moment of inertia, friction coefficients etc.; consequently

$$M(q)\ddot{q} + C(q,\dot{q})\dot{q} + g(q) + A\tau_f = Y(q,\dot{q},\ddot{q})\alpha \qquad (4)$$

where $Y(q,\dot{q},\ddot{q}) \in \mathbb{R}^{n \times n_\alpha}$ is called the regressor matrix, a function of the known generalized coordinates and their first two derivatives, and $\alpha \in \mathbb{R}^{n_\alpha}$ denotes the vector of unknown biped parameters.

Selection of α is not unique, and it is difficult to find minimal set of these parameters [15]. Equation (4) is very important to adaptive control.

3.1.2 The E-L equations of the first kind (the DSP)

As mentioned earlier, the biped mechanism constitutes a closed-chain with over-actuation during the DSP. Therefore, the Lagrange formulation of the 1st kind, which can deals with constraints, is needed for dynamic modeling of the constrained biped. In such case, the motion equations are represented by redundant coordinates resulting in differential algebraic equations DAEs. The algebraic equations result from the constraints derived from the kinematics [16]. The latter can be easily incorporated into the main equations using Lagrange multipliers. The Lagrange equations of the biped robot during the DSP (see Figure 3) can be defined as

$$\frac{d}{dt}\left(\frac{\partial L}{\partial \dot{q}_i}\right) - \frac{\partial L}{\partial q_i} = T_i + \sum_{j=1}^{n_c} \lambda_j \frac{\partial \varphi_j}{\partial q_i} \qquad (i = 1, 2, \ldots\ldots, n_q) \quad (5)$$

where φ_j denotes the constraint function of each closed loop, n_c is the number of these constraints, λ_j is the Lagrange multipliers associated with each constraint. Here n_q is the number of redundant generalized coordinates and equal to the number DOFs (n) of the biped systems plus the number of constraints(n_c).

Equation (5) can be solved using two well-known techniques [17, 18]: the redundant coordinates-based techniques which are used mainly in commercial software such as MSC ADAMS, and the minimum coordinates-based techniques which could be, to some extent, suitable for control strategies and real-time applications. Many researchers have preferred the former technique due to its simplicity and ease of derivation at the expense of difficulties of numerical methods encountered in the solution [17]. Consequently, this motivates the researchers to investigate the second technique which includes eliminating the constraint equations (Lagrange multipliers) from (5) to result in constraint-free differential equations [17]. This can be implemented using one of the orthogonalization methods which are [18]: coordinate partitioning method, zero-eigenvalue method, singular value decomposition (SVD), QR decomposition, Udwadia-Kabala formulation, PUTD method, and Schur decomposition. Solution of (5) results in
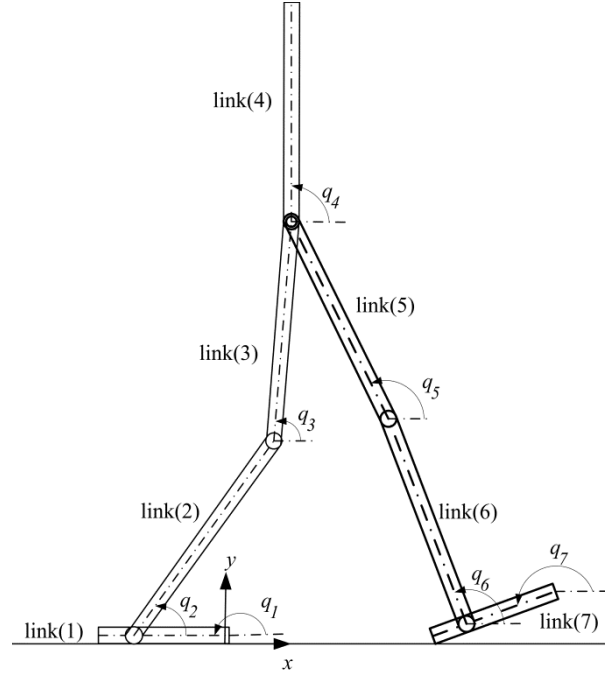
Fig. 3:The biped configuration during the DSP1. In the DSP2 the front foot is fixed and the rear foot rotates.

$$M(q)\ddot{q} + C(q,\dot{q})\dot{q} + g(q) + A\tau_f = A\tau + J^T\lambda \qquad (6)$$

$$\varphi(q) = 0 \qquad (7)$$

with $\varphi \in \mathbb{R}^{n_c}$ is the constraint vector, and $J \in \mathbb{R}^{n_c \times n_q} = \frac{\partial \varphi(q)}{\partial q}$ denotes the Jacobian matrix.

Remark 2. Below we will describe the dynamic analysis for constrained motion of biped robot during the DSP; it is valid for the DSP1 and the DSP2.

Remark 3. The coefficient dynamic matrices (mass matrix, Coriolis and centripetal matrix etc.) of (6) could be determined by the same mathematical formulae defined in the open-chain mechanism.

To reduce the dimension size of (6) (to eliminate λ), a relationship between the redundant generalized coordinates (q) and the independent coordinates ($q_{in} \in \mathbb{R}^n$) should be found. In this thesis, the coordinate partitioning is used for size reduction of the equation of motion [19, 20].

Twice differentiating (7) can result in

$$J(q)\dot{q} = 0 \qquad (8)$$

$$J(q)\ddot{q} + \dot{J}(q,\dot{q})\dot{q} = 0 \qquad (9)$$

Due to the redundancy of coordinates in (6), it is possible to express the dependent generalized coordinates in terms of the independent ones as follows.

$$q_{in} = \breve{\varphi}(q)q \qquad (10)$$

Twice differentiating (10) yields

$$\dot{q}_{in} = J_r(q)\dot{q} \qquad (11)$$

with $J_r(q) \in \mathbb{R}^{n \times n_q} = \frac{\partial \breve{\varphi}(q)}{\partial q}$

$$\ddot{q}_{in} = J_r(q)\ddot{q} + \dot{J}_r(q)\dot{q} \qquad (12)$$

Blocking together (8) and (11) to get

$$\begin{bmatrix} J(q) \\ J_r(q) \end{bmatrix}\dot{q} = \begin{bmatrix} 0 \\ \dot{q}_{in} \end{bmatrix} \qquad (13)$$

Thus, it is possible to get the following important relations

$$\dot{q} = \begin{bmatrix} J(q) \\ J_r(q) \end{bmatrix}^{-1} \begin{bmatrix} \mathbf{0} \\ \dot{q}_{in} \end{bmatrix} = \begin{bmatrix} \breve{F} & F \end{bmatrix} \begin{bmatrix} \mathbf{0} \\ \dot{q}_{in} \end{bmatrix} = F(q)\dot{q}_{in} \qquad (14)$$

The matrix $F \in \mathbb{R}^{n_q \times n}$ plays an important role in eliminating λ; the following orthogonality condition holds

$$J(q)F(q) = \mathbf{0} \qquad (15)$$

Differentiating (14) to obtain

$$\ddot{q} = F(q)\,\ddot{q}_{in} + \dot{F}(q,\dot{q})\,\dot{q}_{in} \qquad (16)$$

Substituting (14) and (16) into (6) to get

$$M(q)\big(F(q)\ddot{q}_{in} + \dot{F}(q,\dot{q})\dot{q}_{in}\big) + C(q,\dot{q})F(q)\dot{q}_{in} + g(q) + A\tau_f = A\tau + J(q)^T\lambda \qquad (17)$$

Alternatively, (17) can be re-written as

$$\bar{M}(q)\ddot{q}_{in} + \bar{C}(q,\dot{q})\dot{q}_{in} + g(q) + A\tau_f = A\tau + J(q)^T\lambda \qquad (18)$$

with

$$\bar{M}(q) = M(q)F(q),\ \bar{C}(q,\dot{q}) = M(q)\dot{F}(q,\dot{q}) + C(q,\dot{q})F(q) \qquad (19)$$

Using (14) and (18) can yield

$$\lambda = \breve{F}(q)^T\big(\bar{M}(q)\ddot{q}_{in} + \bar{C}(q,\dot{q})\dot{q}_{in} + g(q) + A\tau_f - A\tau\big) \qquad (20)$$

Exploiting (15) and pre-multiplying (18) by $F(q)^T$ to obtain

$$F(q)^T\bar{M}(q)\,\ddot{q}_{in} + F(q)^T\bar{C}(q,\dot{q})\dot{q}_{in} + F(q)^T g(q) + F(q)^T A\tau_f = F(q)^T A\tau \qquad (21)$$

Remark 4. Although most researchers have written the matrices, $F(q)$, $\bar{M}(q)$, and $\bar{C}(q,\dot{q})$, in terms of the independent coordinates (q_{in}), these matrices still contain the dependent coordinates (q). Therefore, we have expressed the mentioned matrices in terms of the last coordinates.

Remark 5. The matrix $F(q)$ is not unique; the orthogonalization methods mentioned at the beginning of this subsection are used to get the matrix $F(q)$. Pennesri and Valentini [18] simulated simple pendulum to compare the computational complexity of these orthogonalization methods. QR decomposition ranked best among the other methods. However, all these techniques could be computationally unsuitable to deal with the advanced adaptive control.

Remark 6. Equation (18) has the same properties of that of (2) as follows [21].

Property 4.
Let $D(q) = F(q)^T\bar{M}(q)$, $H(q,\dot{q}) = F(q)^T\bar{C}(q,\dot{q})$, then the matrix $N(q,\dot{q}) = \dot{D}(q,\dot{q}) - 2H(q,\dot{q})$ is skew-matrix.
Proof. Let

$$N = \dot{D} - 2H \qquad (22)$$

By substituting (19) into (22) we get

$$N = \dot{F}^T M F + F^T \dot{M} F + F^T M \dot{F} - 2F^T M \dot{F} - F^T C F = F^T\big(\dot{M} - 2C\big)F + \dot{F}^T M F - F^T M \dot{F} \qquad (23)$$

Since $\dot{M} - 2C$ is skew-matrix according to Property 1, then N is also skew-matrix.

Property 5. The orthogonality condition is satisfied by the matrix $F(q)$ such that (15) holds.
Proof. From (8) and substituting (14), we have

$$JF\,\dot{q}_{in} = \mathbf{0} \qquad (24)$$

Since $\dot{q}_{in}$ is linearly independent, then

$$JF = F^T J^T = \mathbf{0} \qquad (25)$$

Property 6. If $F(q)$ is known, then the left hand side of (18) are linearly dependent on the unknown biped parameters (the same as property 3).

3.1.3 Continuous dynamic response

One of the inherent problems of legged locomotion (bipeds, quadrupeds, etc.) is the discontinuity at the transition instances due to: (i) impact events; these can be avoided by setting the foot velocity to be zero at the instance of contact, and (ii) varying configurations of the biped from the SSP to the DSP and vice versa. As said previously, the number of actuators is more than the DoFs of the biped during the constrained DSP. This means that there are infinity combinations of actuator torque to drive the biped systems as explained below.

One of the methods for determining the actuating torques and the ground reaction forces is the pseudo-inverse matrix as follows.

Equation (6) can be re-arranged to yield

$$M(q)\ddot{q} + C(q,\dot{q})\dot{q} + g(q) + A\tau_f = \begin{bmatrix} A & J(q)^T \end{bmatrix}\begin{bmatrix} \tau \\ \lambda \end{bmatrix} \qquad (26)$$

One of the possible solutions to get the actuating torques and Lagrange multipliers are

$$\begin{bmatrix} \tau \\ \lambda \end{bmatrix} = \begin{bmatrix} A & J^T \end{bmatrix}^{\neq}\big(M(q)\ddot{q} + C(q,\dot{q})\dot{q} + g(q) + A\tau_f\big) \qquad (27)$$

where the notation $[.]^{\neq}$ denotes the pseudo-inverse of the referred matrix.

As seen from (27), there is no guarantee that τ and λ have the same values at the start/end of the SSP due to this optimization solution. Therefore, the following assumption is proposed to resolve this dilemma.

Assumption 4. Because the biped robot does not have a unique solution during the DSP, a linear transition function could be proposed for the ground reaction forces [21-23]. Thus, for the front foot

$$\lambda = \left(\frac{t-t_s}{t_d-t_s}\right) m_G(\ddot{c}_G + [0, g, 0]^T) \qquad (28)$$

where t, t_s and t_d are time parameter, the time of SSP, and the DSP time. Meanwhile, the ground reaction forces, $\bar{\lambda}$, of the rear foot are

$$\bar{\lambda} = m_{COM}(\ddot{r}_{COM} + [0, g, 0]^T) - \lambda \qquad (29)$$

where m_{COM} refers to the center of mass (CoM) of the biped, Accordingly, $\ddot{r}_{COM}$ is the acceleration vector of the biped CoM, and g is the gravity. Accordingly, at the initial instance of DSP, $\lambda = 0$, and the full ground reaction forces are supported by the rear foot, whereas, at the end of the DSP, the full support appears to be in the front foot with $\bar{\lambda} = 0$. On the other hand, because center of gravity (CoG) acceleration of the biped is nonlinear, the resulted ground reaction forces from (28) can generate nonlinear profile despite of multiplication of the latter equation with linear scaling function.

3.2 The modified recursive N-E formulation

Due to computational complexity inherent in the classical Lagrangian formulation, unless it is simplified, the researchers have resorted to the recursive N-E formulation for real time implementation. The philosophy of deriving N-E formulation is different from that of Lagrangian formulation. In the former, the translation/angular equations of motion of each link are derived sequentially using the D'Alembert principle. Due to the coupling effect between each neighbored links and appearance the translation equations of motion, the coupling force wrench appears in the derivation. Then a set of forward and backward recursive equations is used to determine the velocity and force wrenches respectively [15, 8].

However, Fu et al. [8] have shown that the combined identification and control algorithms can be computed in $O(n^3)$ despite using recursive N-E formulation. Strictly speaking, dealing with advanced adaptive control techniques, the recursive N-E formulations could not be powerful; a modification is needed to satisfy the desired target. Zhu [9] exploited the recursive nature of N-E equations to virtually decompose complex robotic systems into subsystems and to use the advanced adaptive techniques recursively. The derivation is exactly of that of recursive N-E formulation, but the difference is that the N-E formulation derive the equation of motion of each link in terms of a frame attached at it first end rather than its CoM.

3.2.1 Derivation of the dynamic equations

Now let us consider a fixed base serial-chain manipulator with revolute and prismatic joints. Thus, the links are numbered from 1 to n_q, where the base link is numbered as zero link. Figure 4 shows link (i) where $i = 1,2, \ldots, n_q$, is connected to other links via mechanical joints at its ends. This link has one driving cutting point associated with the frame $\{T_{i+1}\}$ and one driven cutting point associated with the frame $\{B_i\}$. Thus, the joint (i) has one driven cutting point associated with the frame $\{B_i\}$ and one driving cutting point associated with the frame $\{T_i\}$.
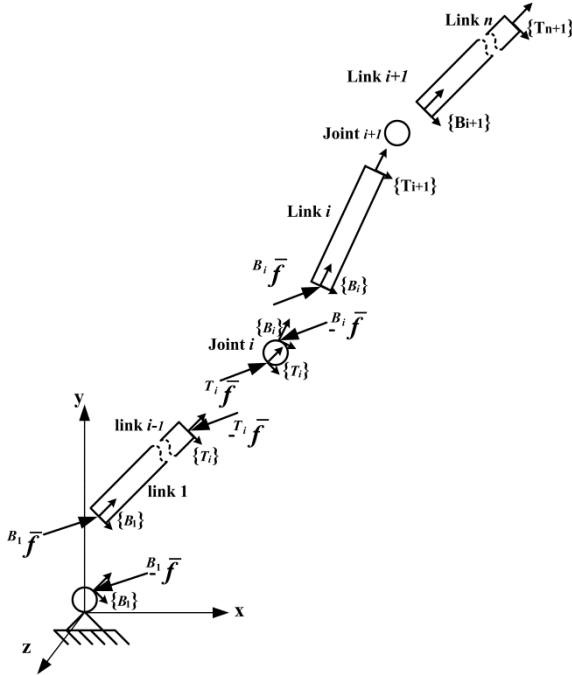

Fig. 4: Virtual decomposition dynamics of a serial-chain manipulator

Below, we will illustrate some definitions and remarks to make the derivation of dynamic equation of each subsystem (link, joint) accessible.

Definition 1 [9]. A cutting point is a directed separation interface that conceptually cuts through a rigid body; the two parts resulting from the virtual cut maintain equal position and orientation. It can be interpreted as a driven cutting point by one part and is simultaneously interpreted as a driven cutting point by another part. Thus, the augmented force/moment vector, $\bar{f} \in \mathbb{R}^6$, (henceforth called the force wrench) is exerted from one part to which the cutting point is interpreted as a driving cutting point to the other part to which the cutting point is interpreted as a drive cutting point.

Remark 7 [9]. The matrix of force wrench transformation, $^B U_A \in \mathbb{R}^{6\times6}$, transforms the force wrench expressed in frame $\{A\}$ to the same force wrench expressed in frame $\{B\}$ as follows.

$$^B\bar{f} = {}^B U_A \; {}^A\bar{f} \tag{30}$$

With

$$^B U_A = \begin{bmatrix} {}^B R_A & \mathbf{0}_{3\times3} \\ ({}^B r_{BA} \times) \, {}^B R_A & {}^B R_A \end{bmatrix} \tag{31}$$

where $^B R_A \in \mathbb{R}^{3\times3}$ refers to the rotation matrix from the frame $\{A\}$ to the frame $\{B\}$, $\mathbf{0}_{3\times3}$ is 3×3 null matrix, $({}^B r_{BA} \times)$ is the skew matrix of the vector $^B r_{BA}$, which represents a vector from the origin of frame $\{B\}$ to the origin of frame $\{A\}$, expressed by

$$\left({}^B r_{BA} \times \right) = \begin{bmatrix} 0 & -{}^B r_{BA)z} & {}^B r_{BA)y} \\ {}^B r_{BA)z} & 0 & -{}^B r_{BA)x} \\ -{}^B r_{BA)y} & {}^B r_{BA)x} & 0 \end{bmatrix} \tag{32}$$

whereas the transpose of $^B U_A$ can transform the velocity wrench from frame to another as follows.

$$^A\bar{v} = {}^B U_A^T \; {}^B\bar{v} \tag{33}$$

Remark 8. The net force wrench of link (i) can be sequentially expressed in terms of frame $\{B_i\}$ as

$$^{B_i}\bar{f}^* = {}^{B_i}\bar{f} - {}^{B_i}U_{T_{i+1}} \; {}^{T_{i+1}}\bar{f} \tag{34}$$

Exploiting Remark 7 to yield

$$^{B_i}\bar{f}^* = {}^{B_i}\bar{f} - {}^{B_i}U_{T_{i+1}} \; {}^{T_{i+1}}U_{B_{i+1}} \; {}^{B_{i+1}}\bar{f} = {}^{B_i}\bar{f} - {}^{B_i}U_{B_{i+1}} \; {}^{B_{i+1}}\bar{f} \tag{35}$$

Remark 9. The velocity wrench of link (i) can sequentially be determined by

$$^{B_i}\bar{v} = z \, \dot{q}_i + {}^{B_{i-1}}U_{B_i}^T \; {}^{B_{i-1}}\bar{v} \tag{36}$$

with $z = [0\,0\,0\,0\,0\,1]$ or $[0\,0\,1\,0\,0\,0]$ for revolute and prismatic joints respectively. Alternatively and simply, the velocity wrench can be calculated as

$$^{B_i}\bar{v} = \begin{bmatrix} {}^{B_i}R_I v_{B_i} \\ {}^{B_i}R_I w_{B_i} \end{bmatrix} \tag{37}$$

with $v_{B_i} \in \mathbb{R}^3$ and $w_{B_i} \in \mathbb{R}^3$ are the absolute translational and angular velocity vector of frame B_i respect to the inertial frame $\{I\}$.

Remark 10. Concerning the target biped, the number of the generalized coordinates (n_q) is always equal to both the number of links, e.g. both the number of links and the generalized coordinates are equal to 6 during the SSP. Consequently, we named the number of links as that of generalized coordinates.

3.2.1.1 Dynamics of link subsystem

By applying the D'Alembert principle to link (i), with respect to the inertial frame about the CoM of link (i), we can get the following relations for the net forces $\bar{f}_i^*$ and the net moment $\bar{m}_i^*$.

$$f_i^* = \frac{d(m_i v_i)}{dt} = m_i \, \dot{v}_i + m_i \, g \tag{38}$$

$$m_i^* = \frac{d(I_i(t)\hat{w}_i)}{dt} = \mathbf{J}_i(t) \, \dot{w}_i + (w_i \times)\mathbf{J}_i(t)w_i = \mathbf{J}_i(t) \, \dot{w}_i + w_i \times (\mathbf{J}_i(t)w_i) \tag{39}$$

where $v_i \in \mathbb{R}^{3\times1}$ refers to the translation velocity vector of each link.

Putting (38) and (39) into block matrix to deal with velocity and force wrenches

$$\begin{bmatrix} m_i \mathbf{I_3} & \mathbf{0}_{3\times3} \\ \mathbf{0}_{3\times3} & \mathbf{J}_i(t) \end{bmatrix}\begin{bmatrix} \dot{\mathbf{v}}_i \\ \dot{\mathbf{w}}_i \end{bmatrix} + \begin{bmatrix} m_i \mathbf{g} \\ (\mathbf{w}_i \times)\mathbf{J}_i(t)\mathbf{w}_i \end{bmatrix} = \begin{bmatrix} \mathbf{f}_i^* \\ \mathbf{m}_i^* \end{bmatrix} \qquad (40)$$

or

$$\begin{bmatrix} m_i \mathbf{I_3} & \mathbf{0}_{3\times3} \\ \mathbf{0}_{3\times3} & \mathbf{J}_i(t) \end{bmatrix}\dot{\bar{\mathbf{v}}}_i + \begin{bmatrix} m_i \mathbf{g} \\ (\mathbf{w}_i \times)\mathbf{J}_i(t)\mathbf{w}_i \end{bmatrix} = \bar{\mathbf{f}}_i^* \qquad (41)$$

with $\mathbf{I_3}$ is 3×3 identity matrix.

Exploiting Remark 7, the net force wrench on the right hand side of (41) can be expressed (transformed) in terms of the frame $\{B_i\}$ as follows.

$$^{B_i}\bar{\mathbf{f}}^* = {}^{B_i}\mathbf{U}_{A_i}{}^{A_i}\bar{\mathbf{f}}_i^* = {}^{B_i}\mathbf{U}_{A_i}\begin{bmatrix} ^{A_i}\mathbf{R}_I & \mathbf{0}_{3\times3} \\ \mathbf{0}_{3\times3} & ^{A_i}\mathbf{R}_I \end{bmatrix}\begin{bmatrix} \mathbf{f}_i^* \\ \mathbf{m}_i^* \end{bmatrix} \qquad (42)$$

In similar manner, the velocity wrench can be represented in terms of the frame $\{B_i\}$ as

$$\bar{\mathbf{v}}_i = \begin{bmatrix} \mathbf{v}_i \\ \mathbf{w}_i \end{bmatrix} = \begin{bmatrix} ^I\mathbf{R}_{A_i} & \mathbf{0}_{3\times3} \\ \mathbf{0}_{3\times3} & ^I\mathbf{R}_{A_i} \end{bmatrix}{}^{B_i}\mathbf{U}_{A_i}^T{}^{B_i}\bar{\mathbf{v}}_i \qquad (43)$$

Differentiating (43) results in

$$\dot{\bar{\mathbf{v}}}_i = \begin{bmatrix} \dot{\mathbf{v}}_i \\ \dot{\mathbf{w}}_i \end{bmatrix} = \begin{bmatrix} (\mathbf{w}_i \times){}^I\mathbf{R}_{A_i} & \mathbf{0}_{3\times3} \\ \mathbf{0}_{3\times3} & (\mathbf{w}_i \times){}^I\mathbf{R}_{A_i} \end{bmatrix}{}^{B_i}\mathbf{U}_{A_i}^T{}^{B_i}\bar{\mathbf{v}}_i +$$

$$\begin{bmatrix} ^I\mathbf{R}_{A_i} & \mathbf{0}_{3\times3} \\ \mathbf{0}_{3\times3} & ^I\mathbf{R}_{A_i} \end{bmatrix}{}^{B_i}\mathbf{U}_{A_i}^T \frac{d}{dt}({}^{B_i}\bar{\mathbf{v}}_i) \qquad (44)$$

Substituting (43) and (44) into (41) results in

$$\mathbf{M}_{B_i}{}^{B_i}\dot{\bar{\mathbf{v}}}_i + \mathbf{C}_{B_i}({}^{B_i}\mathbf{w}_i){}^{B_i}\bar{\mathbf{v}}_i + \mathbf{g}_{B_i} = {}^{B_i}\bar{\mathbf{f}}^* \qquad (45)$$

3.2.1.2 Dynamics of revolute joint subsystem

There are two types of drive transmission systems for robotic joint systems. The first is the direct drive joints, in which the inertia of the motor is included in the corresponding links [9, 15], such that the dynamics of the joint is neglected. The second type of the system deals with a high gear transmission assuming that the inertial forces/torques act along the joint axis [9]. In the latter case, the dynamic equation of the joint (i) can be described as

$$I_{J_i}\ddot{\theta}_i + \mathscr{k}_{ci}\, sign(\dot{\theta}_i) + \mathscr{k}_{vi}\dot{\theta}_i +$$

$$\mathscr{k}_{si}\, sign(\dot{\theta}_i)\exp\left(-\left(\dot{\theta}_i/\eta_{si}\right)\right) + \mathscr{k}_{oi} = \tau_i^* \ (i = 1,2,\dots,n_j) \qquad (46)$$

where I_{J_i} represents the equivalent inertia of the joint (i), $\ddot{\theta}_i$ denote the ith joint acceleration, τ_i^* represents the net torque applied to the joint (i), and n_j denotes the number of joints. The net torque of the joint (i) can be described as

$$\tau_i^* = \tau_{ci} - \mathbf{z}^T{}^{B_i}\bar{\mathbf{f}} \ (i = 1,2,\dots,n_j) \qquad (47)$$

where τ_{ji} is the input control torque of the joint (i) and the second term represents the output torque of the joint (i) towards the link (i).

3.2.2 The SSP

As mentioned earlier, during this walking phase, the biped mechanism is an open chain mechanism with stance foot as fixed link; it should be in full contact with the ground. Therefore, the seven link-biped reduces to 6-link biped during its dynamic analysis. Three important points should be considered carefully when dealing with (45) which are:

    (i)   Determination of velocity wrench.

Solution of the dynamic (45) needs finding the velocity wrench (see Remark 9) which plays an important role in the

adaptive control problem; it can be found as follows. See Figure 5 for clear description of local frames.
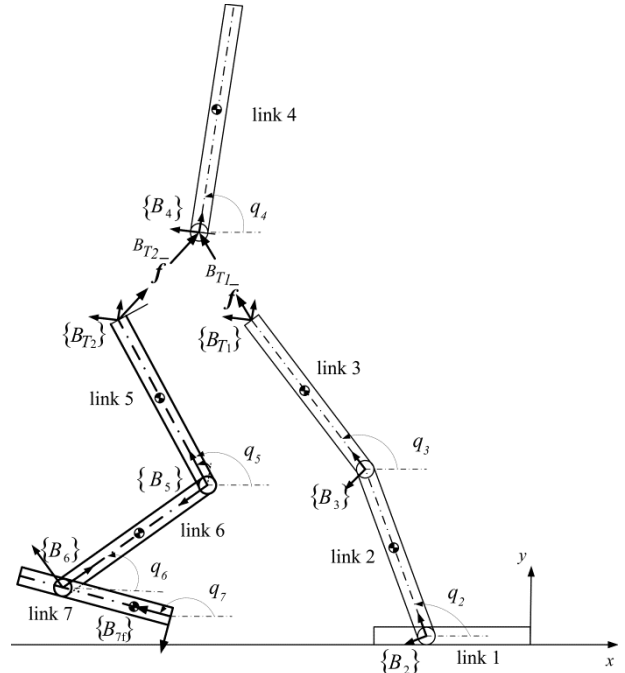

Fig. 5: Biped robot during the SSP with description of assumed local frames

    (ii)   Resultant force wrench

To understand the force wrench distribution at the torso/leg interaction, see Figure 5. Thus, the following relations can be expressed for each link starting from the trunk.

Link (4) (trunk):

$$^{B_4}\bar{\mathbf{f}}^* = {}^{B_{T1}}\bar{\mathbf{f}} + {}^{B_{T2}}\bar{\mathbf{f}} \qquad (48)$$

with notations shown in Figure 5.

Link (5)(swing thigh):

$$^{B_5}\bar{\mathbf{f}}^* = {}^{B_5}\bar{\mathbf{f}} - {}^{B_5}\mathbf{U}_{B_4}{}^{B_{T2}}\bar{\mathbf{f}} \qquad (49)$$

with

$$^{B_5}\mathbf{U}_{B_4} = {}^{B_5}\mathbf{U}_T{}^{B_4}\mathbf{U}_T{}^{-1} \qquad (50)$$

Link (6) (swing shank):

$$^{B_6}\bar{\mathbf{f}}^* = {}^{B_6}\bar{\mathbf{f}} - {}^{B_6}\mathbf{U}_{B_5}{}^{B_5}\bar{\mathbf{f}} \qquad (51)$$

Link (7) (swing foot):

$$^{B_7}\bar{\mathbf{f}}^* = {}^{B_7}\bar{\mathbf{f}} - {}^{B_7}\mathbf{U}_{B_6}{}^{B_6}\bar{\mathbf{f}} \qquad (52)$$

Link (3) (stance thigh):

$$^{B_3}\bar{\mathbf{f}}^* = {}^{B_3}\bar{\mathbf{f}} - {}^{B_3}\mathbf{U}_{B_4}{}^{B_{T1}}\bar{\mathbf{f}} \qquad (53)$$

Link (2)(stance shank):

$$^{B_2}\bar{\mathbf{f}}^* = {}^{B_2}\bar{\mathbf{f}} - {}^{B_2}\mathbf{U}_{B_3}{}^{B_3}\bar{\mathbf{f}} \qquad (54)$$

We note that we have 6 equations for six links (48-54), with 7 unknowns ($^{B_{T1}}\bar{\mathbf{f}}, {}^{B_{T2}}\bar{\mathbf{f}}, {}^{B_5}\bar{\mathbf{f}}, {}^{B_6}\bar{\mathbf{f}}, {}^{B_7}\bar{\mathbf{f}}, {}^{B_3}\bar{\mathbf{f}}, {}^{B_2}\bar{\mathbf{f}}$). Because the swing foot does not have force wrench at the frame $\{B_7\}$, so $^{B_7}\bar{\mathbf{f}} = \mathbf{0}$. Thus, $^{B_6}\bar{\mathbf{f}}$ can recursively be calculated from (52) and so on.

    (iii) Actuating torques

To simplify the analysis, let us assume temporarily that the target biped has direct drive joint systems (the dynamics of

the joint could be neglected [9, 15]) the left hand side of (46) is equal to zero. Consequently, the actuating torques can be calculated from the coupling effect of the neighbored link according to (47) as follows.

Left shank, $\tau_{c1} = \mathbf{z}^T{}^{B_2}\bar{\mathbf{f}}$ (55)

Left knee, $\tau_{c2} = \mathbf{z}^T{}^{B_3}\bar{\mathbf{f}}$ (56)

Left thigh/torso interaction, $\tau_{c3} = \mathbf{z}^T{}^{B_{T_1}}\bar{\mathbf{f}}$ (57)

Right thigh/torso interaction, $\tau_{c4} = \mathbf{z}^T{}^{B_{T_2}}\bar{\mathbf{f}}$ (58)

Right knee, $\tau_{c5} = \mathbf{z}^T{}^{B_5}\bar{\mathbf{f}}$ (59)

Right shank, $\tau_{c6} = \mathbf{z}^T{}^{B_6}\bar{\mathbf{f}}$ (60)

3.2.3 The DSP

Below we will address the problem of over-actuation of the biped during the DSP1. The DSP2 can be dealt with the same procedure of the DSP1; therefore, there is no need to repeat the procedure for the DSP2. As mentioned earlier, the biped in this walking sub-phase, DSP1, has six actuators with 4 DoFs; therefore, two redundant actuators compromise the over-actuation problem. In the following, the details of velocity and force wrenches as well as determining the redundant actuating torques are investigated.

- Velocity wrench. It has exactly the same relations described in previous subsection, with replacing the word (swing) by (front), the word (stance) to (rear), and l_{7a} by $(l_7 - l_{7a})$ for the last link.
- Force wrench. It has also the same force wrenches showed in (48) to (54).
- Actuating torques. We have three significant problems resulting from the variable configurations of the biped which include: (a) redundancy of the actuators, (b) the passive joint on the front foot (see Figure 6) which enforces the torque to be $\tau_{c_f} = 0$, and (c) the discontinuity of the actuating torques. Four solutions are considered below with focus on solutions 3 and 4 which can be ranked best among the rest.
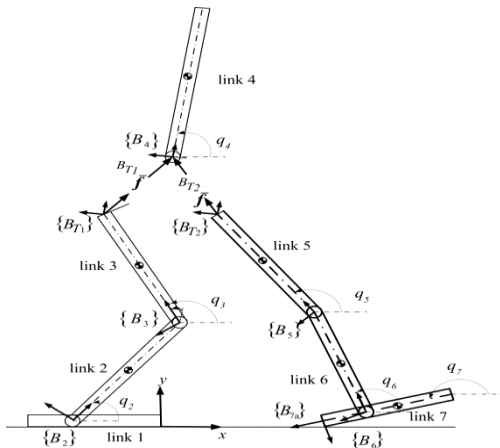

Fig. 6: The biped robot during the DSP1

(i)   Procedure 1-releasing and optimizing the internal forces

This strategy assumes that the biped resembles two cooperating manipulators (two legs) holding one object (the trunk of the biped robot). Thus, the two interaction force wrenches, ${}^{B_{T_1}}\bar{\mathbf{f}}$ and ${}^{B_{T_2}}\bar{\mathbf{f}}$ can be expressed as [9]

$${}^{B_{T_1}}\bar{\mathbf{f}} = \sigma\,{}^{B_4}\bar{\mathbf{f}}^* + \boldsymbol{\eta} \tag{61}$$

$${}^{B_{T_2}}\bar{\mathbf{f}} = (1-\sigma)\,{}^{B_4}\bar{\mathbf{f}}^* - \boldsymbol{\eta} \tag{62}$$

With $\boldsymbol{\eta} \in \mathbb{R}^3$ denotes the internal force wrench and σ is a scalar value bounded by 0 and 1 ($0 \le \sigma \le 1$).

Then, describing the actuating torques in terms of the design variables.

$$\boldsymbol{\tau} = \mathbf{B}_1\boldsymbol{\eta} + \mathbf{b}_1 \tag{63}$$

with the constraint of passive joint

$$\tau_{c_f} = 0 = \mathbf{a}_1{}^T\boldsymbol{\eta} + a_2 \tag{64}$$

By defining the objective function

$$\sigma = \tfrac{1}{2}\,\boldsymbol{\tau}^T\mathbf{W}\boldsymbol{\tau} \tag{65}$$

where $\mathbf{W} \in \mathbb{R}^{6\times 6}$ is a symmetric weighting matrix; it is assumed as an identity matrix in our solution.

Substituting (63) into (65) to get

$$\sigma = \tfrac{1}{2}(\mathbf{B}_1\boldsymbol{\eta} + \mathbf{b}_1)^T\mathbf{W}(\mathbf{B}_1\boldsymbol{\eta} + \mathbf{b}_1) + \mathcal{G}(\mathbf{a}_1{}^T\boldsymbol{\eta} + a_2) \tag{66}$$

Differentiating (66) with respect to $\boldsymbol{\eta}$ and setting it to zero

$$\boldsymbol{\eta} = -(\mathbf{B}_1{}^T\mathbf{W}\mathbf{B}_1)^{-1}\mathbf{B}_1{}^T\mathbf{W}\mathbf{b}_1 - (\mathbf{B}_1{}^T\mathbf{W}\mathbf{B}_1)^{-1}\mathbf{a}_1\,\mathcal{G} \tag{67}$$

Substituting (67) into (64) to yield

$$\mathcal{G} = \frac{a_2 - \mathbf{a}_1{}^T(\mathbf{B}_1{}^T\mathbf{W}\mathbf{B}_1)^{-1}\mathbf{B}_1{}^T\mathbf{W}\mathbf{b}_1}{\mathbf{a}_1{}^T(\mathbf{B}_1{}^T\mathbf{W}\mathbf{B}_1)^{-1}\mathbf{a}_1} \tag{68}$$

Substituting (68) into (67) to get the internal force wrench

$$\boldsymbol{\eta} = -(\mathbf{B}_1{}^T\mathbf{W}\mathbf{B}_1)^{-1}\mathbf{B}_1{}^T\mathbf{W}\mathbf{b}_1 -$$
$$(\mathbf{B}_1{}^T\mathbf{W}\mathbf{B}_1)^{-1}\mathbf{a}_1\left(\frac{a_2 - \mathbf{a}_1{}^T(\mathbf{B}_1{}^T\mathbf{W}\mathbf{B}_1)^{-1}\mathbf{B}_1{}^T\mathbf{W}\mathbf{b}_1}{\mathbf{a}_1{}^T(\mathbf{B}_1{}^T\mathbf{W}\mathbf{B}_1)^{-1}\mathbf{a}_1}\right) \tag{69}$$

Thus, the force wrench at the torso can be determined from (61,62), and sequentially finding the rest force wrenches and the required torques via the following (48-60). The disadvantages of this procedure are that σ is a free parameter; it has not been considered as design variable, and there is also no guarantee to satisfy continuous dynamic response related to actuating torques.

(ii)   Procedure 2- direct optimization of the torso/leg force wrench

Instead of releasing internal force wrench, the actuating torques can directly be expressed in terms of ${}^{B_{T_1}}\bar{\mathbf{f}}$ or ${}^{B_{T_2}}\bar{\mathbf{f}}$. Thus, we can get the same equations above but in terms of ${}^{B_{T_1}}\bar{\mathbf{f}}$ as follows.

$${}^{B_{T_1}}\mathbf{f} = -(\mathbf{B}_1{}^T\mathbf{W}\mathbf{B}_1)^{-1}\mathbf{B}_1{}^T\mathbf{W}\mathbf{b}_1 -$$
$$(\mathbf{B}_1{}^T\mathbf{W}\mathbf{B}_1)^{-1}\mathbf{a}_1\left(\frac{a_2 - \mathbf{a}_1{}^T(\mathbf{B}_1{}^T\mathbf{W}\mathbf{B}_1)^{-1}\mathbf{B}_1{}^T\mathbf{W}\mathbf{b}_1}{\mathbf{a}_1{}^T(\mathbf{B}_1{}^T\mathbf{W}\mathbf{B}_1)^{-1}\mathbf{a}_1}\right) \tag{70}$$

and completing the same steps as of the procedure 1. However, the discontinuity problem has not been resolved in the above two procedures.

(iii)   Procedure 3- tracking desired ground reaction forces. Considering Assumption 4 and assuming the desired reaction force, (28) and (29), as a constraint to yield

$$ {}^{B_7}\bar{\mathbf{f}} = \begin{bmatrix} \lambda \\ \tau_{c_f} \end{bmatrix} = \breve{\mathbf{B}}\,{}^{B_{T_1}}\bar{\mathbf{f}} + \breve{\mathbf{b}} \tag{71}$$

with $\breve{\mathbf{B}} \in \mathbb{R}^{3\times 3}$ and $\breve{\mathbf{b}} \in \mathbb{R}^3$.

The left hand side of (71) is known from the desired walking trajectories, so the problems of over-actuating and discontinuity are solved using the last equation without need of optimization.

Remark 10. If the number of constraints is equal to the design variables, no optimization of the system is necessary because

the solution of equality constraints are the only candidates for the optimum design [24].

(iv)   Procedure 4- tracking desired ground reaction forces with optimization

In this procedure, we will come back to procedure 1 representing the trunk/leg interaction force wrench in terms of the internal force wrench and α parameter. Thus, constraint (71) can be expressed as follows

$$^{B_7}\overline{f} = \begin{bmatrix} \lambda \\ \tau_{c_f} \end{bmatrix} = B_2\eta + b_2\sigma + b_3 \qquad (72)$$

with $B_2 \in \mathbb{R}^{3\times3}$, $b_2 \in \mathbb{R}^3$ and $b_3 \in \mathbb{R}^3$. Re-arranging (72) and using the pseudoinverse definition

$$\begin{bmatrix} \eta \\ \overline{\sigma} \end{bmatrix} = [B_2 \quad b_2]^{\neq}(^{B_7}\overline{f} - b_3) \qquad (73)$$

where $\overline{\sigma}$ denotes the candidate optimal solution. Because of the bounded limits of σ, the following procedure is proposed:

If $0 \leq \overline{\sigma} \leq 1$, then $\sigma = \overline{\sigma}$.

If $\overline{\sigma} \geq 1$, then $\sigma = 1$.

If $\overline{\sigma} \leq 0$, then $\sigma = 0$. $\qquad (74)$

After finding the internal force wrench and α parameter, it is easy to find the actuating torques in a similar way described previously (see procedure 1).

4. CONLUSIONS

In this paper, 6-link biped robot has been modeled using L-E and N-E formulations. The problem of discontinuity is solved using linear transition ground reaction forces without impact-contact event. Lagrangian formulation, unless simplified, could require more computational complexity than that of N-E formulation; the latter can deal with each link separately easing the task of advanced adaptive control. The future work will concentrate on simulation and experiments using two modeling techniques: fixed-base and floating-base biped robot.

5. REFERENCES

[1] Al-Shuka, Hayder F. N.; Corves, B.; Zhu, W.-H.; Vanderborght, B. 2014. Multi-level control of zero-moment point (ZMP)-based humanoid biped robots: A review. Robotica (accepted).

[2] Al-Shuka, H.; Allmendinger, F.; Corves, B.; Zhu, W.-H. 2014. Modeling, stability and walking pattern generators of biped robots: a review. Robotica, 32(06): 907-934.

[3] Sato, T.; Sakaino, S.; Ohnishi, K. 2010. Trajectory planning and control for biped robot with toe and heel joint. IEEE International Workshop on Advanced Motion Control, Nagaoka, Japan, pp.129-136.

[4] Vanderborght, B.; Ham, R. V.; Verrelst, B.; Damme, M. V.; Lefeber, D. 2008. Overview of the Lucy project: Dynamic stabilization of a biped powered by pneumatic artificial muscles. Advanced Robotics: 22 (10), 1027-1051.

[5] Featherstone, R.; Orin, D. 2000. Robot dynamics: Equations and algorithms. IEEE International Conference on Robotics and Automation, ICRA'00, vol. 1, pp. 826-834.

[6] Saha, S. K. 2007. Recursive dynamics algorithms for serial, parallel and closed-chain multibody systems. Indo-US Workshop on Protein Kinematics and Protein Conformations, IISC, Bangalore.

[7] Khalil, W. 2011. Dynamic modeling of robots using recursive Newton-Euler formulations. J. A. Cettoet al.

[8] (Eds.): Informatics in Control, Automation and Robotic, LNEE 89, pp. 3-20, Springer-Verlag Berlin Heidelberg.

[8] Fu, K. S.; Gonzalez, R. C.; C. Lee, S. G. 1987. Robotics: control, sensing, vision, and intelligence. USA: McGraw-Hill Book Company.

[9] Zhu, W.-H. 2010. Virtual decomposition control: towards hyper degrees of freedom. Berlin, Germany: Springer–Verlag.

[10] Al-Shuka, Hayder F. N.; Corves, B. 2013. On the walking pattern generators of biped robot. Journal of automation and control, 1(2): 149-155.

[11] Chen, X.; Watanabe, K.; Kiguchi, K.; Izumi, K. 1999. Optimal force distribution for the legs of a quadruped robot. Machine Intelligence and Robotic Control: 1(2), 87-94.

[12] Hamon, A.; Aoustin, Y. 2010. Cross four-bar linkage for the knees of a planar bipedal robot. 10th IEEE-RAS International Conference on Humanoid Robots, Nashville, TN, pp. 379-384.

[13] Tzafests, S.; Raibert, M.; Robust sliding mode control applied to 5-link biped robot. Journal of Intelligent and Robotic Systems: vol. 15, pp. 67-133.

[14] Li, Z.; Yang, C.; Fan, L. 2013. Advanced control of wheeled inverted pendulum systems. London: Springer-Verlag London.

[15] Spong, Mark. W.; Vidyasagar, M. 1989. Robot dynamics and control. USA: John Wiley & Sons.

[16] Tsai, Lung-Wen. 1999. Robot analysis: the mechanics of serial and parallel manipulators. New York: John Wiley and Sonc Inc.

[17] Blajer, W.; Bestle, D.; Schiehlen, W. 1994. An orthogonal complement matrix formulation for constrained multibody systems. Journal of Mechanical Design: vol. 116.

[18] Pennestri, E.; Valentini, P. P. 2007. Coordinate reduction strategies in multibody dynamics: a review. In Atti Conference on Multibody System Dynamics.

[19] Mitobe, K.; Mori, N.; Nasu, Y.; Adachi, N. 1997. Control of a biped walking robot during the double support phase. Autonomous Robots: 4(3), 287-296.

[20] Su, C.-Y.; Leung, T. P.; Zhou, Q.-J. 1990. Adaptive control of robot manipulators under constrained motion. Proceedings of the 29th Conference on Decision and Control, pp. 2650-2655.

[21] Zarrugh, M. Y. 1981. Kinematic prediction of intersegment loads and power at the joints of the leg in walking. J. Biomechanics: 10 (10), 713-725.

[22] Alba, A. G.; Zielinska, T. 2012. Postural equilibrium criteria concerning feet properties for biped robot. Journal of Automation, mobile robotics and Intelligent Systems: 6 (1), 22-27.

[23] Al-Shuka, Hayder F. N.; Corves, B.; Vanderborght, B.; Zhu, W.-H. 2013. Finite difference-based suboptimal trajectory planning of biped robot with continuous dynamic response. International Journal of Modeling and Optimization, 3(4):337-343.

[24] Arora, J. S. 2012. Introduction to optimum design. USA: Elsevier.